Available online at www.sciencedirect.com
ScienceDirect
Journal of Sound and Vibration 316 (2008) 331–347
JOURNAL OF SOUND AND VIBRATION
www.elsevier.com/locate/jsvi

Localization and quantification of vibratory sources: Application to the predictive maintenance of rolling bearings

X. Chiementin[a,*], F. Bolaers[a], L. Rasolofondraibe[b], J.-P. Dron[a]

[a]*GMMS, Groupe de Mécanique Matériaux et Structures, University of Reims Champagne-Ardenne, BP 1039, 51687 Reims Cedex 2, France*
[b]*CReSTIC, Centre de Recherche en Sciences et Technologies de l'Information et de la Communication, University of Reims Champagne-Ardenne, BP 1039, 51687 Reims Cedex 2, France*

Received 6 July 2006; received in revised form 18 February 2008; accepted 19 February 2008
Handling Editor: C. Morfey
Available online 3 April 2008

Abstract

Among the methods which make it possible to establish a diagnosis on the operating condition of a mechanism, the vibratory techniques seem very promising and are booming. The signals collected by accelerometers are the result of a mixture of various sources each of which corresponds to operation of a component. The diagnosis and monitoring of each component require the determination of the contribution of each source in the signal collected. The objective of this work is to use and optimize the techniques applied to the inverse problems with the aim of quantifying the contribution of each source in the obtained mixture, more particularly, the sources which are characteristic of a damaged element. However, the inverse problems are generally unstable. These instabilities are often related to the errors of measurement or the parasites contained in the signals and require methods of stabilization. This paper proposes a methodology, based on the restitution of the sources. Thus, the methodology ensures the detection and the localization of a defect of a component by the optimization of the position of a limited number of sensors. Two approaches are then proposed: the numerical approach which employs an updated numerical model of the studied structure and the experimental approach based on the correlation between the position of the sensors and the modal parameters of this same structure. The experimental validation of this methodology is carried out on a casing made up of two bearings.

1. Introduction

Predictive maintenance by vibratory analysis makes it possible to increase the productivity and to improve one's performance in terms of reliability, availability and security. This procedure of analysis implements the techniques related to the dynamics of the structures and the signal processing [1,2]. Three levels of analysis are currently used: (i) the monitoring carried out with global indicators, that makes it possible to observe possible drifts of the level of vibrations, (ii) whose diagnosis is aimed at locating a damaged component and (iii) monitoring of the quantification of variation of the failure severity. The vibratory signals resulting from piezoelectric accelerometers represent the response of the structure to various excitations caused by the various

*Corresponding author.
E-mail address: xavier.chiementin@univ-reims.fr (X. Chiementin).

0022-460X/$ - see front matter © 2008 Elsevier Ltd. All rights reserved.
doi:10.1016/j.jsv.2008.02.029

mechanical components. Thus, the aim of our work is to define the contribution of each excitation source in order to quantify its severity. The separation of the sources starting from the measured signal requires the use of inverse problems. However, the inverse problems are ill-posed problems in the sense of Hadamard [3]; they are unstable during the inversion. Many works have studied the inverse problem for the indirect force measurements. We can distinguish two main categories: the first one using mathematical methods and the second one taking into consideration physical phenomena.

The mathematical tools are generally combined with the use of a large number of sensors [4,5]. These sensors give rise to a mixture matrix whose singular value decomposition (SVD) offers a very interesting mathematical base [6]. Within the framework of the vibrations, a first method, described by Powell in 1984 [7], consists in cancelling the lowest singular values considered like noise. Romano [8] decided to reject the singular values lower than 10% of the highest singular value. Elliott [9] and Thite [10] define the threshold according to the level of the uncertainties of the measurements. A second method consists in regularizing these values. This method was implemented by Nelson in 1998 [11] within the field of the indirect measurements of forces, and recently by Kim [12] and Thite [10]. Hansen [13] proposes a method based on the visualization of the solution norm according to the residue. This function forms an L whose corner corresponds to the optimal regularization parameter (the L-curve principle), while Golub [14] proposes a performance index based on the coherences between the measurements, the generalized cross validation (GCV) principle. However, according to Lanczos [15], *A lack of information cannot be remedied by any mathematical trickery*. This statement proves that the regularization methods allow to stabilize the problem but they skew the inversion. Even if the regularization parameter is determined, these regularization methods can delete a source.

The tools, which use the physical phenomena, are inspired by the dynamic structures. Powell [7] shows that two physically very close excitations generate similar deformations, particularly at low frequencies. This fact makes the inversion unstable because of a dependence between the column vectors of the matrix. Fabunmi [16], Hilary [17] and then Desanghere [18] define the existence of a link between the modal analysis of the structure and the number of the determinable sources at a narrow band of frequency. They highlight that the number of modes participating in the response of the structure must be equal or superior to the number of sources. In particular, the restitution of the frequencies close to the resonance frequency is impossible because only one eigenmode governs the structure, and this is all the more true as the structure is lightly damped. Thanks to these remarks, Lee [19], then Hadjit [20], made a measurement selection which allowed to stabilize the inversion. Lee [19] proposes a method based on the maximization of the norm of an undersquared matrix obtained by the SVD. Hadjit [20] defines a new criterion to select the responses by considering the provision of independent information deduced from the matrix of Fischer. Leclère [5] implements a strategy of weighting of the mean squares based on the importance given to each response. It is thus possible to decrease the importance of some vibratory responses positioned on vibration bellies, and to increase the importance if the sensors are positioned on vibration knots. Other works studied the restitution of the frequencies close to the resonance frequency. Lee [19] proposes to add an oscillating system to shift the resonance frequency. This system modifies the structure: consequently, it modifies the resonances. However, this modification can be very important, and it can significantly modify the required sources. Another procedure, implemented by Mas [21], is based on the damping of the structure. Indeed, a damped structure has less acute resonance peaks, which improve the stability.

This paper is inspired by these works, in order to implement the restitution of the sources related to the damage of one or several components. However, some of the points are different from the previous studies. The nature of the quantities to be restored are "accelerations", whereas the previous studies propose the restitution of the forces. The reasons are that restored accelerations can be compared to measured ones and that the measured quantities and the quantities to restore have the same order of magnitude. Then, we wish to use a limited number of sensors and to optimize the restitution in narrow bands of frequencies around characteristic frequencies of bearing defects. The objective is not to increase the *quantity* of the information but the *quality* (given by the sensors). The previous studies have implemented a selection among several sensors but they did not propose a mathematical model to optimize the position of the sensors. They describe only some principles (a global repartition, to avoid a vibration knot). This is why this work determines a relation between the modal parameters and the position of the observations giving place to conditioning maps. These maps define the positions of the sensors. This relation avoids using the regularization methods which

can delete sources, and the use of a narrow band of frequency avoids the resonance frequency. The method described is compared to the regularization method using the L-curve principle. We established the effectiveness of this method on a case which contains two main bearings.

2. Linear inverse problems in vibratory analysis

Inverse problems make it possible to restitute sources from observations. As far as we are concerned, they allow to determine the vibratory sources from measurements realized by sensors. For this, knowledge of the mathematical model of the direct problem is essential. The responses of a structure, $y_i(t)$, are the convolution products of the source time history, $x_j(t)$, by the structure impulse $t_{i,j}$, Eq. (1). In our case, the source time history and the responses are parameters with the same unity, i.e. accelerations

$$y_i(t) = \Sigma_{j=1}^{p} t_{i,j}(t) * x_j(t), \quad i = 1, \ldots, m \tag{1}$$

where p is the number of sources and m is the number of responses. $*$ is the convolution product. This expression is simplified in the frequency domain where it becomes a simple linear product,

$$\mathbf{Y}(\omega) = \mathbf{T}(\omega).\mathbf{X}(\omega) \tag{2}$$

where $\mathbf{Y}(\omega)$, $\mathbf{X}(\omega)$ and $\mathbf{T}(\omega)$ are, respectively, the vector of the responses, the vector of the sources and the transmissibility matrix. To compute $\mathbf{X}(\omega)$, the problem, apparently simple, is to reverse the matrix $\mathbf{T}(\omega)$. However, the inversion suffers from instability which we are going to explain. This work uses the SVD which transforms the transmissibility matrix,

$$\mathbf{T} = \mathbf{U}.\Sigma.\mathbf{V}^H \tag{3}$$

where $\mathbf{U} = (u_1, \ldots, u_p)$ and $\mathbf{V} = (v_1, \ldots, v_m)$ are the orthogonal matrices of type (p,p) and (m,m). $\mathbf{V}^H$ is the Hermitian transpose of $\mathbf{V}$. Σ is a diagonal matrix whose elements are the singular values σ_i of matrix $\mathbf{T}$. The orthogonal vectors v_k are known as the right singular vectors, and, the orthogonal vectors u_k are known as the left singular vectors.

Without additive noise, sources are computed directly by inversing the mixture matrix, Eq. (4). However, a linear system is often perturbed by noise. This is why the sources are computed thanks to a least squares approach. The sources $\mathbf{X}$ are chosen so that the $\mathbf{T}.\mathbf{X}$ is as close as possible to $\mathbf{Y}$,

$$\mathbf{X} = \mathbf{V}.\Sigma^{-1}.\mathbf{U}^H\mathbf{Y} \Rightarrow \min(\|\mathbf{Y} - \mathbf{T}.\mathbf{X}\|) \tag{4}$$

2.1. Experimental and numerical constraints of inversion methods

Generally, the inversion methods are ill-posed problems, because the stability of the inversion is hard to satisfy, whereas a well-posed problem satisfies three criteria [3]: the uniqueness, the existence and the stability of the solution. Small errors on response data generate important errors on computed sources. If the matrix can be reversed, the errors on $\mathbf{X}$, $\delta\mathbf{X}$, are defined by [22]

$$\frac{\|\delta\mathbf{X}\|}{\|\mathbf{X}\|} \leqslant c(\mathbf{T})\left(\frac{\|\delta\mathbf{T}\|}{\|\mathbf{T}\|} + \frac{1}{\cos\theta}\frac{\|\delta\mathbf{Y}\|}{\|\mathbf{Y}\|}\right) + c(\mathbf{T})^2 \tan\theta \frac{\|\delta\mathbf{T}\|}{\|\mathbf{T}\|} \tag{5}$$

where $c(\mathbf{T})$ is the condition number defined by

$$c(\mathbf{T}) = \|\mathbf{T}\|\|\mathbf{T}^{-1}\| \tag{6}$$

The angle θ measures the gap between the vectors $\mathbf{Y}$ and $\mathbf{TX}$, in other words, the size of the residue, $\|\mathbf{Y} - \mathbf{TX}\|$. Thus, if the residue (or θ) is low, the "actual" conditioning is similar to $c(\mathbf{T})$; on the contrary, if the residue is relatively high, the conditioning is in the order of $c(\mathbf{T})^2$. Finally, if θ is close to $\pi/2$, the solution is much lower than the residue; the "actual" conditioning becomes unbounded even if $c(\mathbf{T})$ is low. Reasonably, we consider

that the residue is low, thus, Eq. (5) is simplified,

$$\frac{\|\delta \mathbf{X}\|}{\|\mathbf{X}\|} \leqslant c(\mathbf{T})\left(\frac{\|\delta \mathbf{T}\|}{\|\mathbf{T}\|}+\frac{\|\delta \mathbf{Y}\|}{\|\mathbf{Y}\|}\right) \tag{7}$$

This relation shows that the restitution errors mainly depend on the conditioning of the mixture matrix. A high condition number signifies a badly conditioned matrix, and a low condition number signifies a well-conditioned matrix. Thus, the inversion is stable for a small condition number.

To improve the stability and the quality of the inversion method, there are numerous methods that we have mentioned in the introduction. Our aim is to suggest an optimal position of a limited number of sensors. The suggestions will be compared with a regularization method proposed by Tikhonov [23], associated with the L-curve principle [24] indicating the value of the regularization parameter. This regularization consists in minimizing a performance index J_β, Eq. (8), which replaces the minimization given by Eq. (4)

$$J_\beta = \min(\|\mathbf{Y}-\mathbf{T}\mathbf{X}\|^2+\beta\|\mathbf{X}\|^2) \tag{8}$$

The term $\|\mathbf{Y}-\mathbf{T}\mathbf{X}\|$ represents errors between the measured and computed responses. The second term is the norm of input vectors with a weighting parameter β, obtained by a graphical method. The norm $\|\mathbf{X}\|$ is represented according to $\|\mathbf{Y}-\mathbf{T}\mathbf{X}\|$ in log–log. This curve forms an L whose angle corresponds to the optimal value β.

3. Development of stabilization approaches

3.1. Inversion quality and numerical approach

3.1.1. Conditioning map

Historically, this approach was the first to be highlighted. The origin of this approach is a simple questioning about the existence of areas where the position of the sensors would be favorable to the stability of the inversion. According to the previous paragraph, a small condition number signifies a stable inversion. However, the condition number depends on the mixture matrix, i.e., on the structure, and on the position of the sensors and the sources. This is why the numerical approach generates maps of structure representing the isovalues of condition numbers. These maps are called ''conditioning maps'', and they are determined for a narrow band of frequency. Thus, the optimal positions are directly determined to make a stable inversion.

3.1.2. Procedure of the numerical approach

This approach requires a numerical model of the studied structure. The position of one sensor is regarded as being a variable, while the other sensors are fixed on the structure. This variable sensor scans all the nodes. For each node of the structure, the condition number is computed. Thus, good positions are highlighted and the conditioning map is determined.

3.2. Inversion quality and experimental approach

3.2.1. Condition number and modal analysis

By definition, the condition number is written as

$$c(\mathbf{T}) = \|\mathbf{T}\|\|\mathbf{T}^{-1}\| \tag{9}$$

Hence

$$c(\mathbf{T}) = \frac{1}{\|\det(\mathbf{T})\|}\|\mathbf{T}\|\|\mathrm{Com}(\mathbf{T})^t\| \quad \text{with } \mathbf{T}^{-1} = \frac{\mathrm{Com}(\mathbf{T})^t}{\det(\mathbf{T})} \tag{10}$$

$\mathrm{Com}(\mathbf{T})^t$ is the transpose of the adjugate matrix $\mathbf{T}$. The relation in Eq. (7) shows us that we must obtain a condition number close to 1 to reduce the propagation of the errors. However, this relation remains directly unusable. We can simplify the problem and declare that the inversion will be stable if the denominator, $\det(\mathbf{T})$, is different from zero. This hypothesis requires an experimental validation which will be realized in the

following sections. In such a case, Chiementin [25] has explained the relations between modal analysis and the determinant of the matrix: if the number of dominant modes is lower than the sources, the condition number is infinite, then the inversion is impossible. On the contrary, we have Eqs. (11) and (12), respectively, for a number of sources equal to 2 and for a number of sources superior to 2

$$\left\| \sum_{j,k=1;j<k}^{M} \frac{1}{D_j D_k} [\phi_j(x_1)\phi_k(x_2) - \phi_j(x_2)\phi_k(x_1)][\phi_j(y_1)\phi_k(y_2) - \phi_j(y_2)\phi_k(y_1)] \right\| \neq 0 \tag{11}$$

with

$$D_l = -\omega^2 M_l + \mathrm{i}\omega C_l + K_l$$

where M_l, C_l and K_l are the lth diagonal terms of the matrix of mass, of stiffness and of damping, expressed in the modal base. ϕ_i is the eigenvector i. M is the number of dominant modes or the number of the modes participating in the response, in the studied spectral band. x_i and y_i are, respectively, the source i and the observation i

$$\begin{aligned}
&\left\| \sum_{k_1,k_2,\ldots,k_p=1}^{M} \frac{1}{D_{k_1} \cdots D_{k_p}} \Phi(x,k_1,\ldots,k_p).\Phi(y,k_1,\ldots,k_p) \right\| \neq 0, \quad k_1 < k_2 < \cdots < k_p, \quad \forall i,\ k_i\ \varepsilon\ \mathbb{N} \\
&\text{where } \Phi(x,k_1,\ldots,k_p) = \sum_{\substack{i=1\ to\ p \\ j=0,1}} (-1)^j \phi_{k_1}(x_{i+(p-1)j})\phi_{k_2}(x_{i+1+(p-3)j}) \cdots \phi_{k_p}(x_{i+(p-1)+(p-(2p-1))j}) \\
&\text{where } \Phi(y,k_1,\ldots,k_p) = \sum_{\substack{i=1\ to\ p \\ j=0,1}} (-1)^j \phi_{k_1}(y_{i+(p-1)j})\phi_{k_2}(y_{i+1+(p-3)j}) \cdots \phi_{k_p}(y_{i+(p-1)+(p-(2p-1))j}) \\
&\text{The indexes for } x \text{ and } y \text{ are modulo } p,\ p \geqslant 3
\end{aligned} \tag{12}$$

where the terms $\Phi(x,k_1,\ldots,k_p)$ represent the sources, and the terms $\Phi(y,k_1,\ldots,k_p)$ represent the observations.

3.2.2. Procedure of the experimental approach

Thanks to the established inequality, the determinant of transmissibility matrix and the eigenmodes are linked. This link makes it possible to increase the inversion stability. The principle is to use a limited number of sensors by positioning them correctly. We have established an experimental procedure to determine the optimal areas for the positioning of the sensors:

- to carry out the modal analysis of the structure;
- to determine the number of dominant modes for each characteristic frequency;
- to use the inequalities in Eqs. (11) and (12) by taking into account the possible simplifications, in order to find optimal positions
- to position sensors in well-conditioned areas, thanks to the inequality determined.

4. Numerical and experimental validation

4.1. Definitions

We define "a real source", the physical cause which can excite the structure (a rolling bearing in this work). Thus, a real source can contain one or several defects. We define "a virtual source", denoted as x, the setting where the measured signal is the result of the operating state of only one real source. An observation, denoted as y, is the setting where the measured signal is the result of the simultaneous operation of the real sources. Thus, the position of a virtual source can be the position of an observation.

4.2. Description of the test bench

The studied structure is a module laid out on a test platform originally made within a contract between the state (France) and the region Champagne-Ardenne, called "SURVIB", SURveillance of industrial machines by VIBratory diagnosis. This platform is composed of a concrete frame on which a steel-grooved plate is incorporated, two modules with motors of 10 kW and modules to ensure study of mechanical components (a module of detection for rolling bearings, a module of detection for gears, a module of fatigue for rolling bearings, a module of fatigue for gears). The studied module is the module of detection for rolling bearings, Fig. 1a. The module is composed of two 6206 rolling bearings which play the part of real sources. The rotation is realized thanks to a motor module with a speed of rotation of 1500 rev/min. The two bearings are radially loaded thanks to hydraulic jacks with a force of 5000 N.

The numerical model was realized thanks to a finite element software. The casing is composed of 17,000 solid elements with 8 nodes and the shaft is realized with a 20 beam element, Fig. 1b. The rolling bearings are integrated thanks to a toolbox realized and explained by Debray [26]. This toolbox is based on the model suggested by DeMul, [27], which integrates the centrifugal forces in the resolution of the problem of static balance of the bearings. The bearing is modeled with three types of elements: (i) Rigid beam elements with two nodes, which model the incompressibility of the inner ring (IR) on the shaft. These elements connect the neutral fiber of the shaft to the nodes of contact between the IR and the rolling elements. (ii) Beam elements with two nodes, whose stiffness matrices are determined by iterations (model of DeMul), by solving the problem of nonlinear balance related to the contacts between the rolling elements and the rings (theory of Hertz) under the effect of the external loads applied. Each ball is thus modeled by an element with two nodes. (iii) Lastly, the shell elements with 4 nodes represent the outer ring (OR) and operate the junction between the elements with two nodes characterizing the rolling elements and the solid elements chosen for the casing. These elements transmit all of the degrees of freedom to the casing. The numerical model is updated by minimizing the performance index, $f_{\text{objective}}$,

$$f_{\text{objective}} = \sum_j \left(\left(\frac{f_{\text{id}j} - f_{\text{num}j}}{f_{\text{id}j}} \right)^2 + \left(\frac{MAC_{j,j} - 100}{100} \right)^2 \right) \tag{13}$$

where

$$\text{MAC}_{i,j}(\phi_{\text{num}_i}, \phi_{\text{exp}_j}) = \frac{\|\phi^H_{\text{num}_i} \phi_{\text{exp}_j}\|^2}{\|\phi^H_{\text{num}_i} \phi_{\text{num}_i}\| \|\phi^H_{\text{exp}_j} \phi_{\text{exp}_j}\|} \tag{14}$$

where $f_{\text{id}j}$ and $f_{\text{num}j}$ are, respectively, the jth identified frequency and the jth numerical frequency. ϕ_{num_i} and ϕ_{exp_j} are, respectively, the numerical eigenvectors and the eigenvectors determined by the modal analysis. The diagonal matrix MAC is the modal assurance criterion. It defines the orthogonality of the modes. We can see that the first resonance frequency for the casing is of 470 Hz. This frequency has an important role in the dominance of the modes.

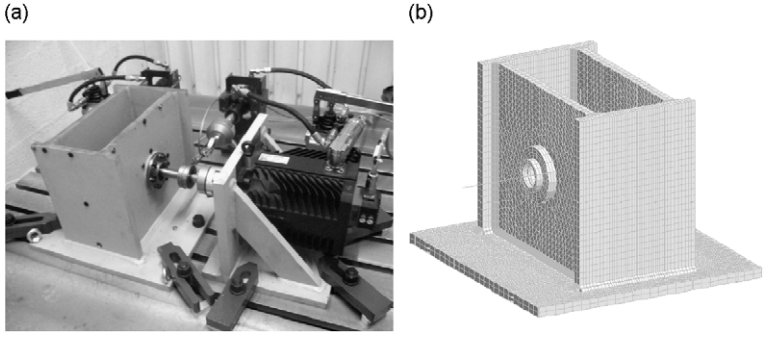

Fig. 1. (a) Test bench, module of detection with rolling bearings; (b) updated model.

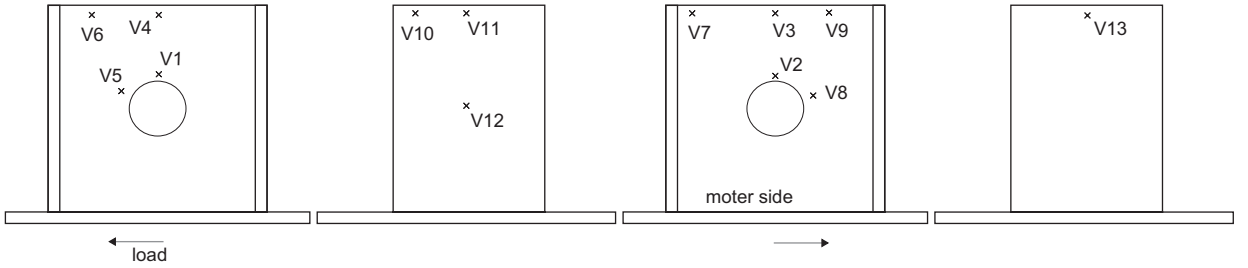

Fig. 2. Instrumentation of the test bench.

The casing is instrumented to record 13 signals (Fig. 2). The 13 positions are denoted as V1–V13. The direction of the load is symbolized by an arrow. These different channels will allow to test the areas which are badly or well conditioned. There is no radial position because the shaft bearing is supposed to be inaccessible. The signals are collected by data acquisition, Siglab, with 8192 points and with several sampling rates. The spectra are obtained with an average of 10 acquisitions.

4.3. Real sources/virtual sources/observations

The real sources are the two rolling bearings. Each can have a defect on the OR, on the IR, on a ball or on the cage. The first two defects are the most frequent, which is why we only study those. For a speed rotation of 1500 rev/min, the potential characteristic frequencies are 89.2 Hz for OR and 135.8 Hz for IR. These values are given by the kinematics of the structure and by the geometry of the rolling bearing. As the number of real sources are 2, two virtual sources are necessary. We highlight that the position of the virtual sources is not always the setting where the exciting force is applied. We choose two virtual sources, whose positions are, respectively, V1 and V2 (Fig. 2). The number of observations can be deduced from the number of real sources; i.e. 2. A higher number of observations will be used in the following section in order to compare the proposed approaches and the regularization methods. The first observation is selected in V3; the second is optimized for the potential characteristic frequencies thanks to the proposed methods.

4.4. Numerical approach

The first approach consists in using an updated numerical model. We use the procedure described in Section 3.1.2. A sensor is fixed at V3 (Fig. 2). The second sensor scans all the nodes of the model. Thus, the transmissibility matrix and the condition number are computed for each position. All the condition numbers are reported in a "conditioning map" which is visualized by MEDIT[1] This map is realized for the characteristic frequencies of the potential defects, i.e. 89.2 and 135.8 Hz (Fig. 3). The two maps obtained are very similar and they show us areas of stability which are common. The similarity between these maps proves that there is a frequency band where the dominant modes are identical. Indeed, the numerical study has shown us that the maps are similar up to 380 Hz, whereas the first resonance frequency is of 470 Hz. This allows us to have just one map for the 0–380 Hz band called "global map". Thus, we can stabilize the inversion for the characteristic frequencies and for several harmonics (178.4, 267.6, 356.8 Hz).

Let us note that the experiment has shown that a good conditioning number is lower than 20. The conditioning map describes areas where this condition is satisfied. The sensor must be placed in these areas, called "well conditioned areas". On the contrary, the other areas must be avoided.

4.5. Experimental approach

The experimental approach is based on the procedure described in Section 3.2.2.

[1]Conceived and realized by the laboratory Jacques Louis Lions of the University Pierre et Marie CURIE.

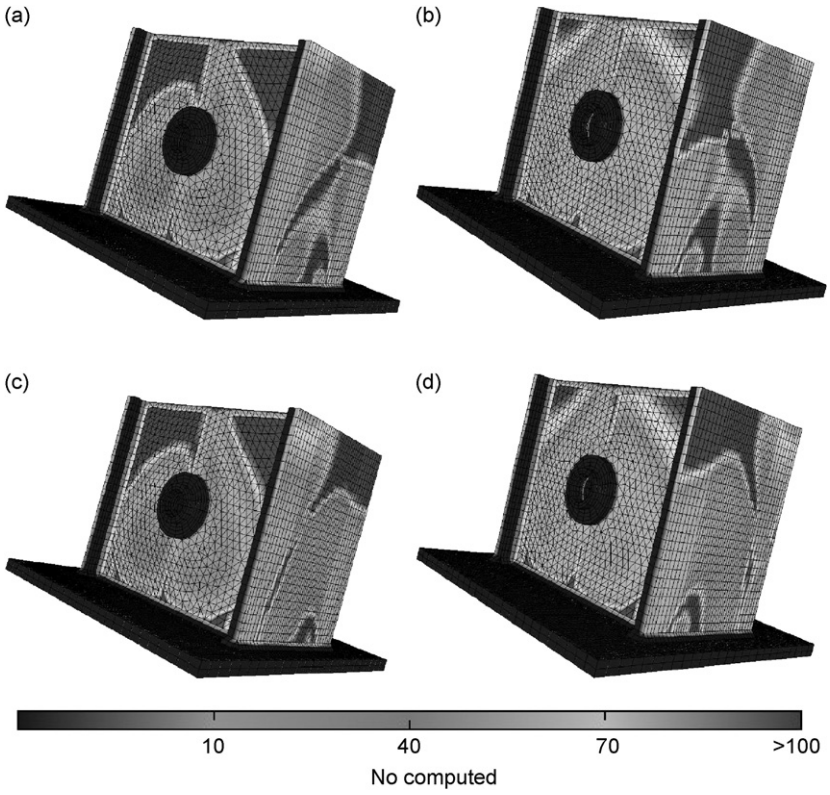

Fig. 3. Conditioning map for (a,c), 89 Hz, (b,d) 115 Hz. (a,b) Front view 3/4, faces 1 and 2. (c,d), Back view 3/4, faces 3 and 4.

4.5.1. Research of the dominant modes

At first, we search the dominant modes. For this, we express the terms of the transmissibility matrix. These terms are the transmissibility functions, deduced from the traditional transfer function, Eq. (15). They are defined like the linear combination of eigenmodes [25], Eq. (16)

$$h_{x_j \to y_i}(\omega) = \sum_{k=1}^{n} \frac{\phi_k(x_j)\phi_k(y_i)}{-\omega^2 M_k + i\omega C_k + K_k} = \frac{D(y_i)}{F(x_j)} \tag{15}$$

where $F(i)$, $D(i)$ and $A(i)$ are, respectively, the force, the displacement and the acceleration in the frequency domain for the i node.

$$\begin{aligned} t_{x_j \to y_i}(\omega) &= \frac{A(y_i)}{A(x_j)} = \frac{-\omega^2 D(y_i)}{-\omega^2 D(x_j)} = \frac{D(y_i)}{F(x_j)} . \frac{F(x_j)}{D(x_j)} = \frac{h_{x_j \to y_i}(\omega)}{h_{x_j \to x_j}(\omega)} \\ &= \frac{\sum_{k=1}^{M} \dfrac{\phi_k(x_j)\phi_k(y_i)}{-\omega^2 M_k + i\omega C_k + K_k}}{\sum_{k=1}^{M} \dfrac{\phi_k(x_j)\phi_k(x_j)}{-\omega^2 M_k + i\omega C_k + K_k}} \\ &= \sum_{k=1}^{M} a_k(x_j, \omega)\phi_k(y_i) \end{aligned} \tag{16}$$

As x_j corresponds to a fixed position, $t_{x_j \to y_i}$ only depends on y_i. We can say that the determination of $a_k(x_j, \omega)$ allows to evaluate the contribution of each term. This determination simplifies the Eq. (16) to M'

terms ($M' \leqslant M$). The contribution of each eigenmode is directly deduced,

$$\%\ \text{contribution}_p = \frac{\|a_p(x_i,\omega)\|}{\sum_{k=1}^{M}\|a_k(x_i,\omega)\|} \tag{17}$$

To determine these contributions, we have performed a modal analysis which makes it possible to obtain the modal parameters. These parameters are used to create a numerical model by expansion [28] thanks to the SDT Toolbox of Balmès [29]. Then, the obtained model is excited through the nodes which represent the interface between the rolling bearing and the casing in order to determine the transmissibility function. This excitation is in the direction of the load.

The quadratic difference between the displacements obtained thanks to the excitation and the linear combination of the modal deformations gives us the contribution of each mode. Table 1 shows us that these contributions are almost similar for the two characteristic frequencies and a limit frequency of 380 Hz. This computation shows that two modes are dominant, 4 and 5, with a percentage of 54.6% and of 33.2%.

4.5.2. Conditioning maps

Secondly, we determine the optimal positions thanks to the expression, Eq. (11). The previous paragraph reveals the dominance of two modes. Thus, the problem comes down to a problem with 2 dominant modes, 2 sources and 2 observations ($M = 2$, $p = 2$). The inequality in Eq. (12) is simplified in Eq. (18)

$$\|(\Phi_4(x_1)\Phi_5(x_2) - \Phi_4(x_2)\Phi_5(x_1))(\Phi_4(y_1)\Phi_5(y_2) - \Phi_4(y_2)\Phi_5(y_1))\| \neq 0. \tag{18}$$

This inequality has two variables: $\Phi_4(y_2)$ and $\Phi_5(y_2)$. The other terms are constant. The eigendeformations provide us with important information to simplify the inequality, (Fig. 4). The first term of the inequality is different from zero because the eigendeformations give $\Phi_4(x_1) = -\Phi_4(x_2)$ and $\Phi_5(x_1) = \Phi_5(x_2)$, and hence:

$$\begin{aligned}\|\phi_4(x_1)\phi_5(x_2) - \phi_4(x_2)\phi_5(x_1)\| &= \|\phi_4(x_1)\phi_5(x_2) + \phi_4(x_1)\phi_5(x_2)\| \\ &= \|2\phi_4(x_1)\phi_5(x_2)\| \\ &\neq 0\end{aligned} \tag{19}$$

Table 1
Contribution of each mode to the vibratory response

	Mode 4 (%)	Mode 5 (%)	The others (%)
Contribution (for 89 Hz)	54.6	33.2	12.2
Contribution (for 115 Hz)	52.8	31.5	15.7
Contribution (for 380 Hz)	57.1	35.7	7.2

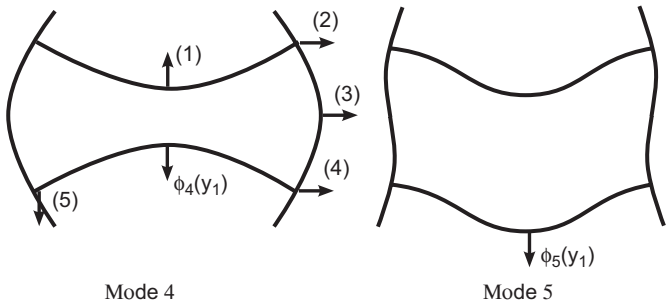

Fig. 4. Eigendeformations of modes 4 and 5, top view.

The position of the sources is not detrimental to the stability of the inversion, and so, the position of the sensors is defined by the relation:

$$\|\phi_4(y_1)\phi_5(y_2) - \phi_4(y_2)\phi_5(y_1)\| \neq 0. \tag{20}$$

In order to determine these optimal positions, several cases, which are indicated by numbers in Fig. 4, are considered.

- The observation number 2 is positioned near the first observation: the eigendeformations are almost equal, and so, Eq. (18) is canceled which creates a high condition number. This number is lower if the observation number 2 moves away. This means that the observation number 2 must be preferably positioned on another face of the casing.
- The observation number 2 is positioned in (1): in this case we have $\phi_4(y_1) = -\phi_4(y_2)$ and $\phi_5(y_2) = \phi_5(y_1)$, so $\phi_4(y_1)\phi_5(y_2) - \phi_4(y_2)\phi_5(y_1) = 2\phi_4(y_1)\phi_5(y_1) \neq 0$. The conditioning will also be good.
- The observation number 2 is positioned in (3): $\phi_5(y_2) = 0$, so $\phi_4(y_1)\phi_5(y_2) - \phi_4(y_2)\phi_5(y_1) = -\phi_4(y_2)\phi_5(y_1) \neq 0$. The conditioning will be good.
- The observation number 2 is positioned in (5): $\phi_5(y_2) = 0$ and $\phi_4(y_2) = 0$ $\phi_4(y_1)\phi_5(y_2) - \phi_4(y_2)\phi_5(y_1) = 0$. The conditioning will be bad.
- The observation number 2 is positioned in (2) or (4): the difference seems to be unimportant because the eigendeformations are almost similar but this example is more difficult to interpret. In (2), the condition number will be good but not in (4). Mathematically, we have the following equalities: $\phi_4(y_2)_{(2)} = \phi_4(y_2)_{(4)}$ and $\phi_5(y_2)_{(2)} = -\phi_5(y_2)_{(4)}$. Thus, the inequality is not checked in case (4).

According to these different cases, we can state that it is sometimes difficult to interpret the well-conditioned areas. Certain cases, like point (1) or (3), are easy to study. On the contrary, the difference between (2) and (4) is more difficult to interpret. We can state that the face with the second source is a well-conditioned area. We can add that the face with the first sensor must be avoided. This fact is logical: in practice, we would not position the two sensors on the same face. The optimal positions deduced from the experimental approach correspond to those obtained by the numerical approach. From now on, we can validate the concept of the conditioning map by the restitution of the sources.

4.6. *Restitution of the sources...*

The two rolling bearings have a defect on the OR with a surface of 8 mm^2 and a defect on the IR with a surface of 20 mm^2, whose characteristic frequencies are, respectively, 89.2 and 135.8 Hz for the speed rotation of 1500 Hz. These defects have been generated by sparking erosion. They have an elliptic form to simulate the distribution of the pression resulting from the contact between the rotating components determined by the Hertz theory. We want to highlight the influence of the sliding which penalizes the restitution. Indeed, the spectral peaks can slide off some frequential points. This is why it is necessary to make the measurements with considerable precaution, to avoid these phenomena.

The temporal signals of the two virtual sources are presented in Fig. 5. The spectra of the virtual sources, determined in Fig. 6, shows us all the characteristic frequencies of the defects, i.e. 89.2, 178.4, 267.6 and 356.8 Hz, except the frequency at 135.8 Hz certainly due to the axial position of the virtual sources.

4.6.1. *...from a well-conditioned area, WCA*

The approaches proposed in this paper consist in positioning the second sensor in V4 for example. In this case, we have temporal and spectral signals, respectively, in Figs. 7 and 8. Thus, the temporal signals of the observations are the result of 4 defects from two rolling bearings. Let us note that the spectra do not have all the characteristic frequencies. The peak for the frequency 135 Hz does not exist on the spectrum of observation 2. For the 4 spectra of the virtual sources and of the observations, we distinguish two characteristic frequencies close to 270 Hz (the second harmonic of the defect IR and the third harmonic of the defect OR).

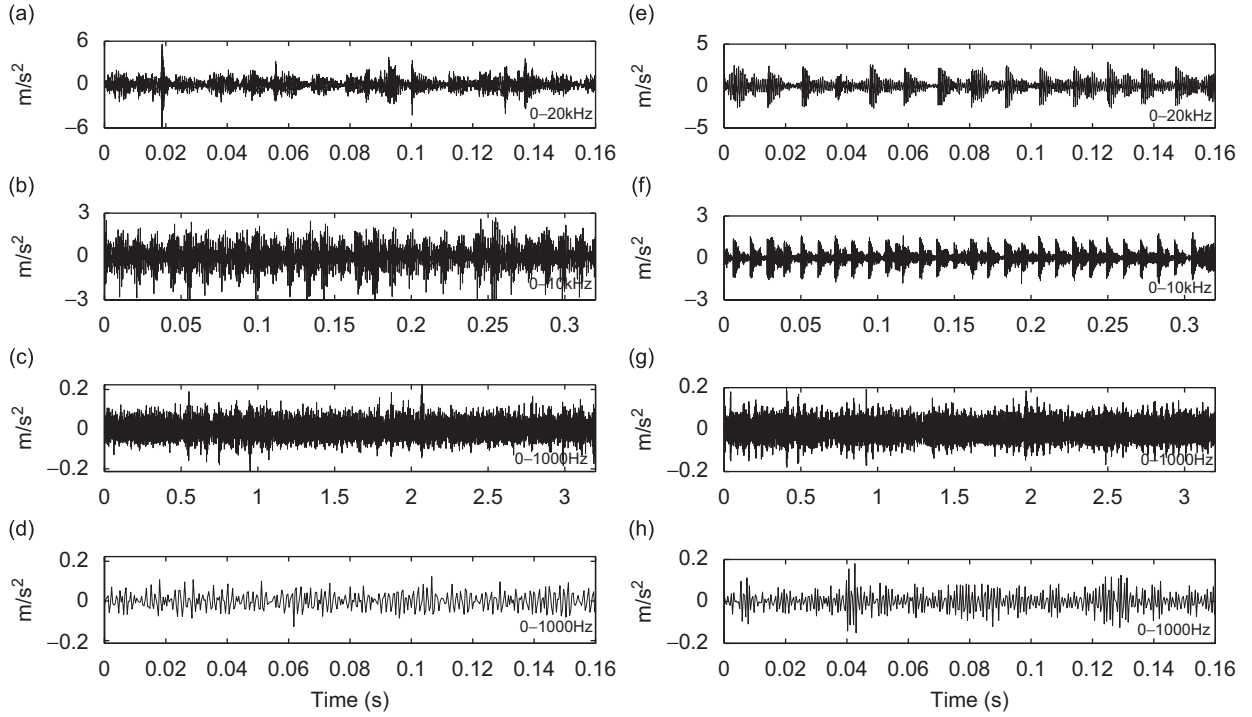

Fig. 5. Temporal signals of the measured virtual sources, V1 and V2. Source 1 (V1) sampled at : (a) 51,200 Hz, (b) 25,600 Hz, (c) 2560 Hz and (d) 2560 Hz zoom on 0.16 s. Source 2 (V2) sampled at (e) 51,200 Hz, (f) 25,600 Hz, (g) 2560 Hz and (h) 2560 Hz zoom on 0.16 s.

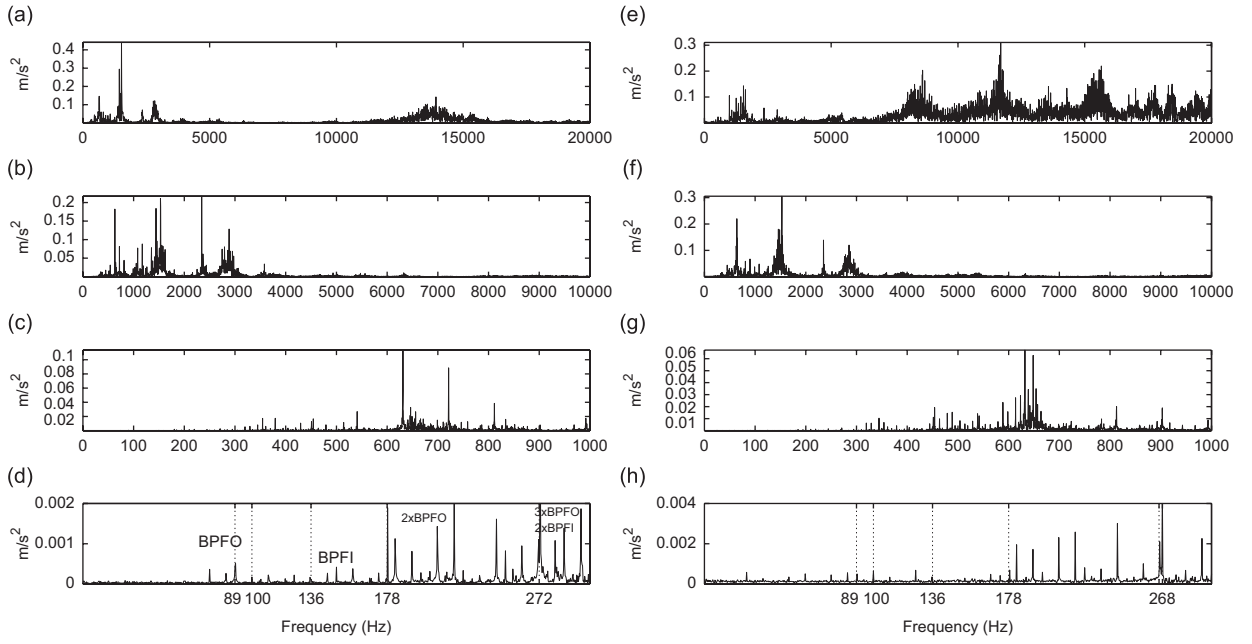

Fig. 6. Spectra of the measured virtual sources, V1 and V2. Spectra of the source 1 (V1) on (a) 0–20,000 Hz, (b) 0–10,000 Hz, (*c*) 0–1000 Hz and (d) 0–300 Hz. Spectra of the source 2 (V2) on (e) 0–20,000 Hz, (f) 0–10,000 Hz and (g) 0–1000 Hz and (h) 0–300 Hz.

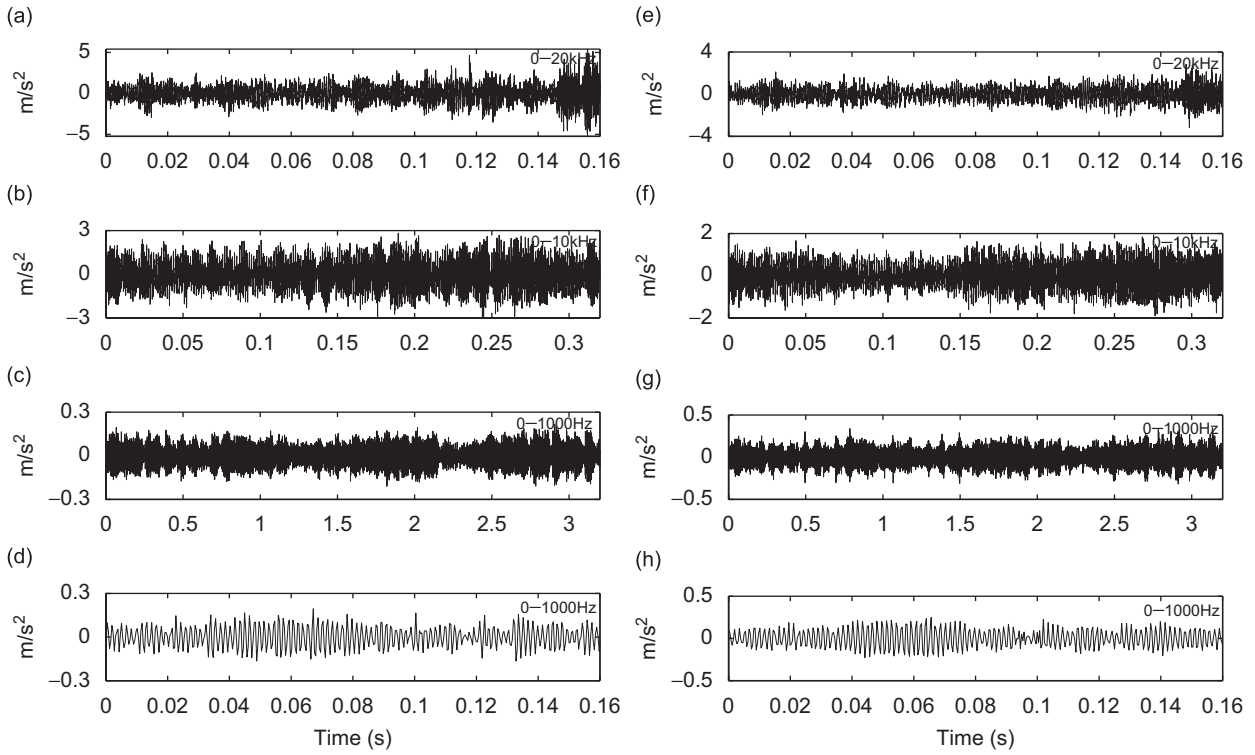

Fig. 7. Signals of the observations. Observation 1 (V3) sampled at (a) 51,200 Hz, (b) 25,600 Hz, (c) 2560 Hz, (d) 2560 Hz zoom on 0.16 s. Observation 2 (V4) sampled at (e) 51,200 Hz, (f) 25,600 Hz, (g) 2560 Hz and (h) 2560 Hz zoom on 0.16 s.

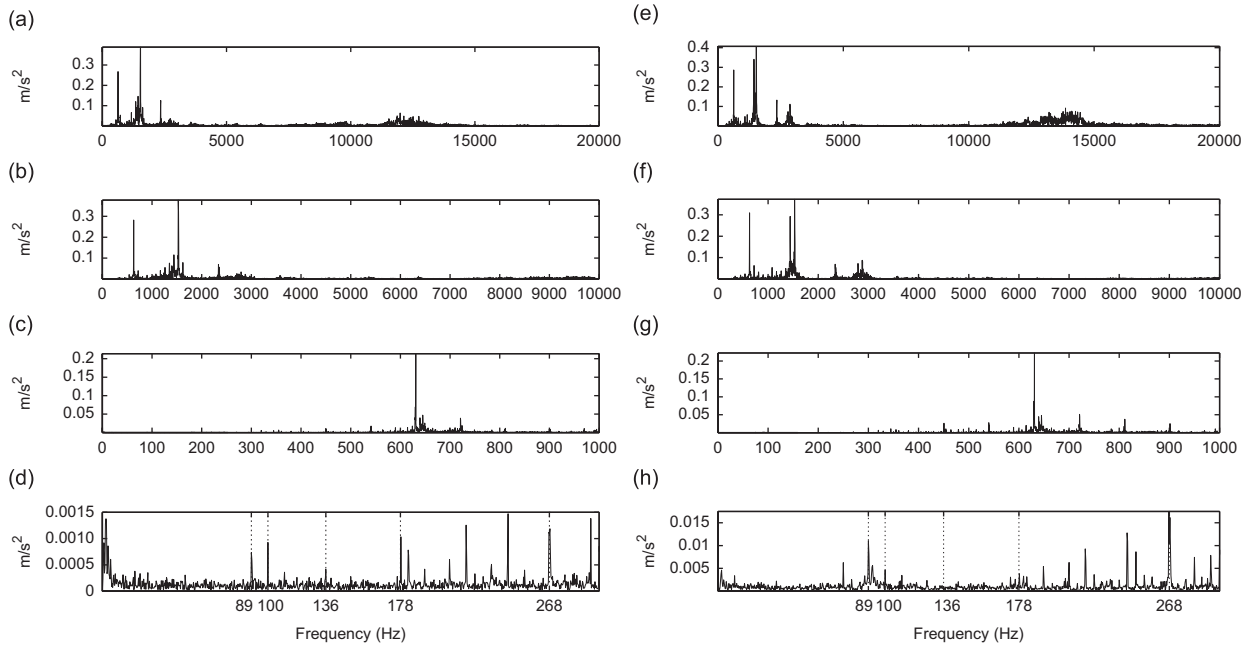

Fig. 8. Spectra of the observations. Spectra of observation 1 (V3) on: (a) 0–20,000 Hz, (b) 0–10,000 Hz, (c) 0–1000 Hz, (d) 0–300 Hz. Spectra of observation 2 (V4) on (e) 0–20,000 Hz, (f) 0–10,000 Hz, (g) 0–1000 Hz and (h) 0–500 Hz.

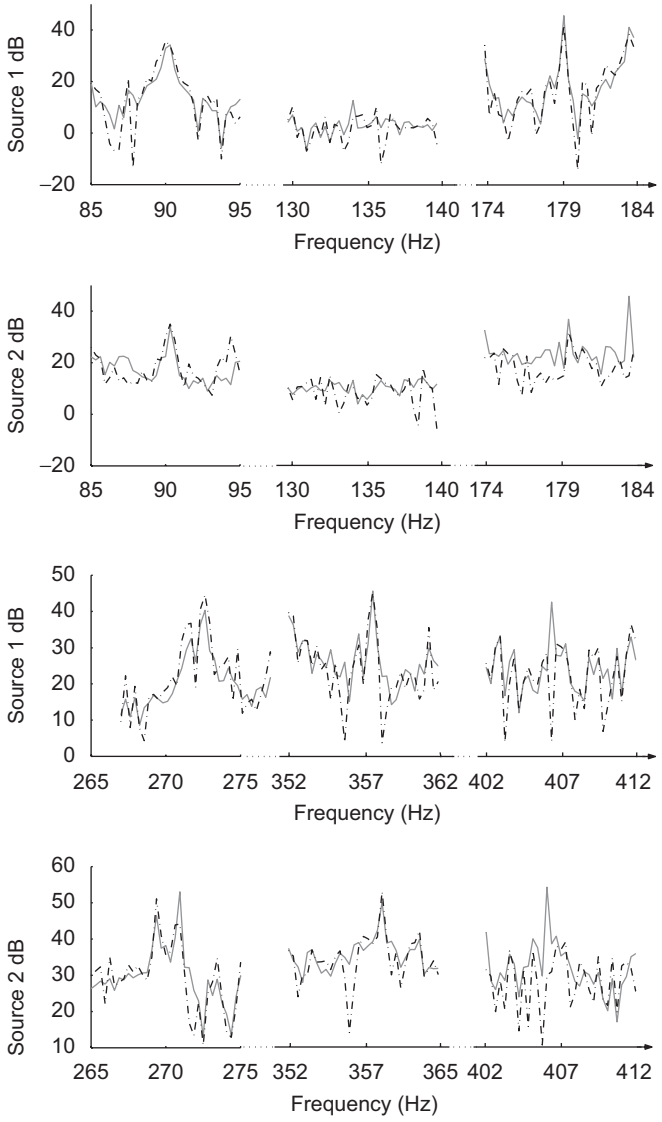

Fig. 9. Restitution of the fundamentals and of the harmonics from a WCA. (—) measured virtual sources, (-.-) restored virtual sources.

The restitutions, Fig. 9, show good results for the characteristic frequencies included between 0 and 380 Hz; the errors do not exceed the value 3.1%. However, the frequency of 405 Hz is prone to a bad restitution. Let us note that the detection of a defect on IR is realized with only one harmonic because the fundamental on the chosen virtual sources does not exist. This fact can be criticized for a reliable diagnosis.

4.6.2. ...from a badly conditioned area, BCA

From now on, we will perform a restitution from a badly conditioned area to show the necessity of a well-conditioned area. For this, we choose the channel V6. The results of the restitution, Fig. 10 and Table 2, reveal huge errors of restitution which do not allow to diagnose the presence of defects. The defect on IR is impossible to diagnose for the rolling bearing 2 (source 2), because the fundamental frequency of 135.8 Hz does not exist because of the positions of the sources and the harmonic at 370 Hz is not well restituted. The defect on OR can be diagnosed on source 1 thanks to the fundamental and two harmonics: while we cannot diagnose this defect on the second source, the characteristic frequencies are not well restituted or not restituted at all.

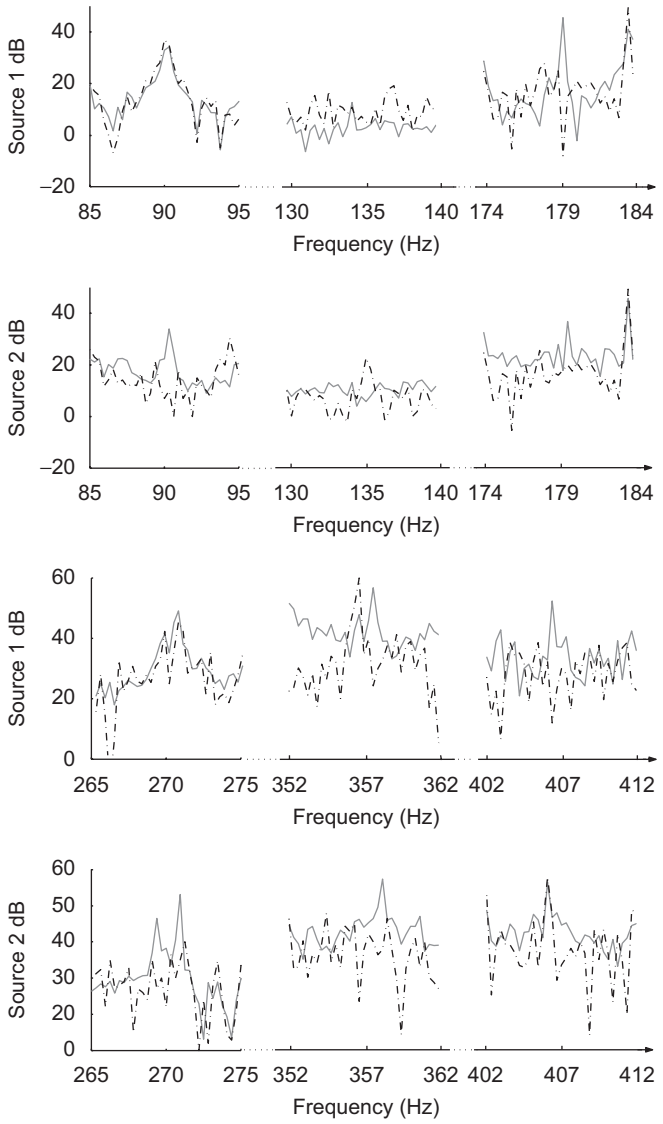

Fig. 10. Restitution of the fundamentals and of the harmonics from a BCA. (—) measured virtual sources, (-.-) restored virtual sources.

4.6.3. ...with an overdetermined system

The seven measurements, V3–V13, create the observation vector. The L-curve is plotted for a range of β in Fig. 11. Thus, the regularization parameter β is determined, $\beta = 8.3$. The results of restitution are presented in Fig. 12 and in Table 2. The defects on OR and IR can be diagnosed on the two sources, even if there are some errors of restitution for some characteristic frequencies: the fundamental at 90 Hz on source 2 and the second harmonic at 270 Hz. The quantification of each frequency is acceptable; the maximal error is 15.1%. We can see that the diagnosis of the defect on IR on source 1 is not reliable because the restituted harmonic at 270 Hz can correspond to the defect on OR and not to the defect on IR. Finally, we can highlight that the harmonic at 405 Hz is well restituted for the two sources while this frequency is not in the stipulated frequency band by our two proposed approaches.

4.6.4. Intermediary conclusion

The results of the restitution of the sources show the usefulness of the well-conditioned areas. This optimization proves to be more efficient than the overdetermined methods with a regularization. But it is true that the proposed

Table 2
Comparisons between the methods; ∞ signifies not restituted

WCA	89.2 Hz BPFO	135.8 Hz BPFI	178.4 Hz 2xBPFO	267.6 Hz 3xBPFO	271.6 Hz 2xBPFI	356.8 Hz 4xBPFO	407.4 Hz 3xBPFI
Error x_1 (%)	+0.9	–	−2.3	+1.1	+0.9	+1.5	∞
Error x_2 (%)	–	−2.8	0.2	+2.2	−3.1	+3.0	∞
BCA	89.2 Hz	135.8 Hz	178.4 Hz	267.6 Hz	271.6 Hz	356.8 Hz	407.4 Hz
Error x_1 (%)	0.3	–	∞	−5.6	−10.2	+50.1	∞
Error x_2 (%)	∞	–	∞	∞	∞	∞	9
Overdetermined	89.2 Hz	135.8 Hz	178.4 Hz	267.6 Hz	271.6 Hz	356.8 Hz	407.4 Hz
Error x_1 (%)	0.1	–	−9.8	∞	−3.3	+2.2	−15.1
Error x_2 (%)	–	–	+1.2	+9.2	−4.5	+14.7	−12.2

$$\text{Error}(\%) = \frac{\|x_{\text{obs}} - x_{\text{res}}\|^2}{\|x_{\text{obs}}\|^2} 100$$

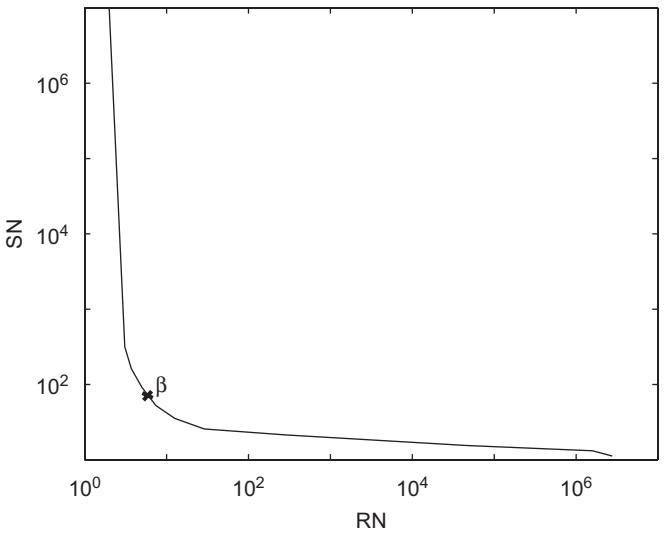

Fig. 11. L-curve principle, determination of the regularization parameter.

approaches can appear to be difficult to use if we do not have a numerical model. Table 3 summarizes the advantages and the disadvantages of our proposed approaches and of the overdetermined method.

5. Conclusions

This work fits into the scheme of a predictive maintenance by vibratory analysis. The aim is to separate the contribution of the different vibratory sources recorded by a sensor. Thus, the inverse problems are implemented within the framework of the quantification and the localization of the vibratory defects. In particular, this paper introduced two approaches to stabilize the inversion of a linear problem in vibratory analysis. These two approaches are based on the optimization of the position of a limited number of sensors in order to locate and to quantify the vibratory sources linked to the damage of the rolling bearings. The optimization criterion is the condition number or the determinant of the matrix of transmissibility. The first approach is a numerical approach which requires a numerical model of the structure. It consists in computing the condition number for each configuration of sensors, and all the results give a conditioning map showing us the optimal areas. The second approach is an experimental approach that uses experimental modal analysis. An inequality is developed whose the resolution gives the optimal

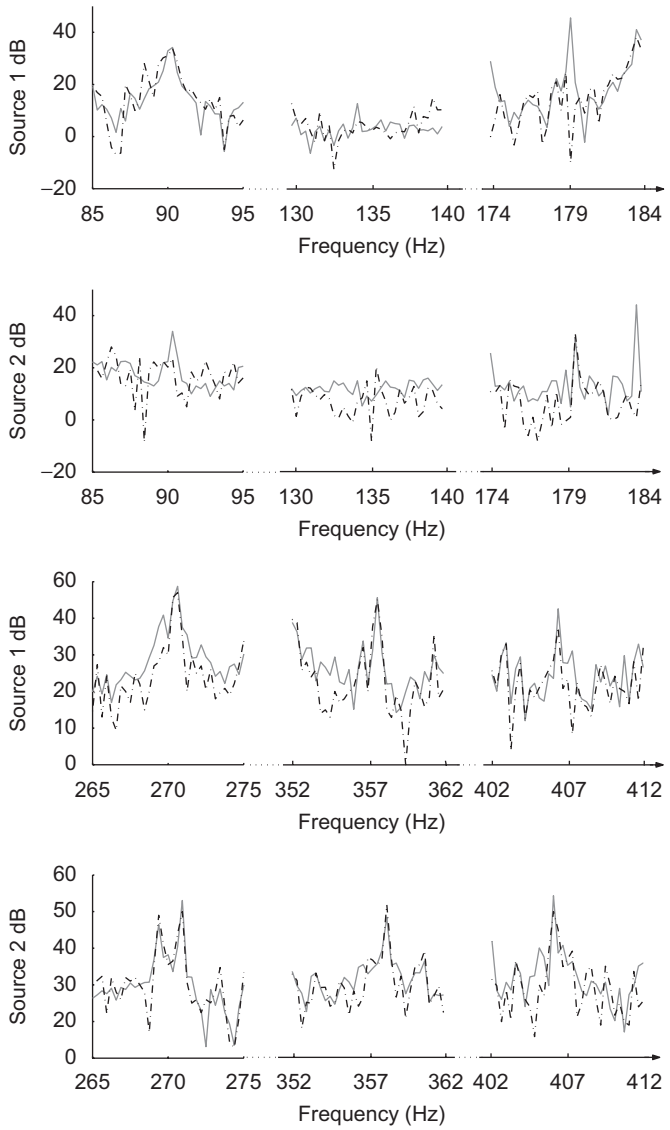

Fig. 12. Restitution of the fundamentals and of the harmonics with an overdetermined system. (—) measured virtual sources, (-.-) restored virtual sources.

Table 3
Comparisons between the regularization method and the proposed approaches

	Regularization with the L-curve method	Sensor position
Sensor's number	Large number	Equal to sources
Restitution	In large band	In narrow band
Restitution stability	Good	Very good
Implementation	Easy	Difficult

positions. The use of these approaches is validated by restoring the vibratory sources arising from damaged rolling bearings. Comparison with a method using an overdetermined system combined with a regularization method reveals the validity of the proposed approaches.

Acknowledgments

The authors wish to thank the region (Champagne-Ardenne) and the state (France) for their financial assistance through the state-region project "SURVIB".

References

[1] A. Jardine, D. Lin, D. Banjevic, A review on machinery diagnostics and prognostics implementing condition-based maintenance, *Mechanical Systems and Signal Processing* 20 (2005) 1483–1510.
[2] P. McFadden, J. Smith, Vibration monitoring of rolling element bearings by the high-frequency resonance technique-a review, *Tribology International* 17 (1984) 3–10.
[3] J. Hadamard, Sur les problèmes aux dérivées partielles et leur signification physique, Princeton University Bulletin (1902) 49–52.
[4] C. Pezerat, T. Loyau, J. Guyader, Characterisation of vibration sources on a set of plates using the riff technique, *Noise Control Engineering Journal* 50 (2) (2002) 50–57.
[5] Q. Leclère, C. Pezerat, B. Laulagnet, L. Polac, Indirect measurement of main bearing loads in an operating diesel engine, *Journal of Sound and Vibration* 286 (1–2) (2005) 341–361.
[6] G. Golub, W. Kahan, Calculating the singular values and pseudo-inverse of a matrix, *Journal of the Society for Industrial and Applied Mathematics: Series B, Numerical Analysis* 2 (2) (1965) 205–224.
[7] R. Powell, W. Seering, Multichannel structural inverse filtering, *Journal of Vibration, Acoustics, Stress, and Reliability in Design* 106 (1984) 22–28.
[8] J. Romano, J. Lopez, Practical application of transfer path analysis to resolve structure-borne noise problems in vehicle design, *Proceedings of ISMA* vol. 21, Leuven, Belgium, 1996.
[9] K. Elliott, J.-N. Juang, J. Robinson, Force prediction using singular value decomposition, *Proceedings of IMAC*, Kissimmee, FL, USA, 1988.
[10] A. Thite, D. Thompson, The quantification of structure-borne transmission paths by inverse methods: part 1: improved singular value rejection methods, *Journal of Sound and Vibration* 264 (2003) 411–431.
[11] P. Nelson, S. Yoon, Estimation of acoustic source strength by inverse method: part 1: conditioning of the inverse problem, *Journal of Sound and Vibration* 233 (4) (2000) 639–664.
[12] J. Kim, T. Waters, P. Nelson, Numerical modelling of vibration sources in hard disk drive by inverse methods, *Proceedings of the International Conference on Structural Dynamic Modelling*, Funchal, Portugal, 2002.
[13] P. Hansen, Analysis of discrete ill-posed problems by means of the l-curve, *SIAM Review* pp. 561–580.
[14] G.-H. Golub, M. Heath, G. Wahba, Generalized cross-validation as a method for choosing a good ridge parameter, *Technometrics* 21 (2) (1979) 215–223.
[15] C. Lanczos, *Linear Differential Operators*, Van Nostrand Reinhold Ed., New York, 1961.
[16] J. Fabunmi, Effects of structural modes on vibratory force determination by the pseudo-inverse technique, *AIAA Journal* 24 (3) (1986) 504–509.
[17] B. Hillary, D. Ewins, The use of strain gauges in force determination and frequency response function measurements, *Proceedings of IMAC* 2, Orlando, FL, USA, 1984.
[18] G. Desanghere, Identification and Quantification of Noise and Vibration Sources using Frequency Response and Coherence Functions, PhD Thesis, Katholieke Universiteit, Leuven, Belgium, 1987.
[19] J. Lee, Y.-S. Park, Response selection and dynamic damper application to improve the identification of multiple input forces of narrow frequency band, *Mechanical System and Signal Processing* 8 (6) (1994) 649–664.
[20] R. Hadjit, Méthodes Inverses Adaptées à l'identification de forces d'excitation de Structures Mécaniques, PhD thesis, Faculté Polytechnique de Mons, 2001.
[21] P. Mas, P. Sas, K. Wyckaert, Indirect force identification based upon impedance matrix inversion: a study on statistical and deterministical accuracy, *Proceedings of ISMA*, vol. 19, Leuven, Belgique, 1994.
[22] G.-H. Golub, C. Loan, *Matrix Computations*, Johns Hopkins University, 1996.
[23] A. Tikhonov, V. Arsenin, *Solutions of Ill-posed Problems*, W.H. Winston, Washington, DC, 1977.
[24] H. Busby, D. Trujillo, Optimal regularization of an inverse dynamic problem, *Computers and Structures* 63 (2) (1997) 243–248.
[25] X. Chiementin, F. Bolaers, L. Rasolofondraibe, J.-P. Dron, Inverse approach for the restitution and the localization of vibratory sources, *Journal of Vibration and Control* 13 (8) (2007) 1169–1190.
[26] K. Debray, F. Bogard, Y. Guo, Numerical vibration analysis on defect detection in revolving machines using two bearing models, *Archive of Applied Mechanics* 74 (1–2) (2004) 287–314.
[27] J.D. Mul, J. Vree, D. Maas, Equilibrium and associated load distribution in ball and roller bearings loaded in 5 degrees of freedom while neglecting frictions: part i: general theory and application to ball bearings, *Journal of Tribology* 111 (1) (1989) 142–148.
[28] E. Balmès, Sensors, degrees of freedom, and generalized modeshape expansion methods, *International Modal Analysis*, 1999, pp. 628–634.
[29] E. Balmès, *Structural Dynamics Toolbox: User's guide*, Version 4, Scientific Software Group, 2000.